Int. J. Nano Dimens., 9 (3): 238-245, Summer 2018

ORIGINAL ARTICLE

Preparation and characterization of friendly colloidal Hydroxyapatite based on natural Milk's casein

Reyhaneh Sahba[1]; Mirabdullah Seyed Sadjadi[1,]; Ali Akbar Sajjadi[2]; Nazanin Farhadyar[3]; Babak Sadeghi[4]*

[1]*Department of Chemistry, Science and Research Branch, Islamic Azad University, Tehran, Iran*
[2]*Institute of Water and Energy, Sharif University of Technology, Tehran, Iran*
[3]*Department of Chemistry, Veramin Branch, Islamic Azad University, Veramin, Iran*
[4]*Department of Chemistry, Tonekabon Branch, Islamic Azad University, Tonekabon, Iran*

Received 10 January 2018 revised 14 March 2018; accepted 27 April 2018; available online 28 April 2018

Abstract

Biocompatible hydroxyapatite nanocomposites are biocompatible, biodegradable, nontoxic and have been paid many attentions as one of the most suitable vehicle for drug delivery use. Our objective in this work was to prepare and characterize caseins based HA nanocomposite in a colloidal form for drug delivery purposes. Casein biopolymer was firstly extracted from skimmed milk by adding acetic acid and was used then to prepare colloidal hydroxyapatite nanoparticles (nHA) through a modified microemulsion technique. Characterization of the as prepared samples was carried out by means of Fourier Transform Infrared (FT-IR) spectroscopy, X-ray powder diffraction patterns (XRD), Field Emission Scanning and Transmission Microscopy (FESEM & TEM). Dynamic light scattering (DLS) technique was finally used to measure particle size and zeta potential distribution of the sample using electrophoresis mobility. The results revealed successful preparation of a colloidal HA /casein suspension with a hydrodynamic zeta average particle size distribution of 256.6 nm.

Keywords: *Casein Micelle; Colloidal Hydroxyapatite; Degradable Biopolymer; Dynamic Light Scattering, Micro Emulsion Technique*

How to cite this article

Sahba R, Seyed Sadjadi M, Sajjadi AK, Farhadyar N, Sadeghi B. Preparation and characterization of friendly colloidal Hydroxyapatite based on natural Milk's casein. Int. J. Nano Dimens. 2018; 9 (3): 238-245.

INTRODUCTION

Many nanoparticle systems have been used and studied as potential candidates in the release, drug delivery and bioimaging purposes. A very good example in this area was hydroxyapatite nanoparticle (nHA) which is a natural source of calcium for human body being as a dispersed colloidal system of calcium phosphate with a size correlated to the colloidal calcium phosphate in milk's casein micelles [1]. Construction and in vivo application of these kind controlled drug delivery systems is one of the most important scientific activities due to their direct relationships with human health care. In this work, we specifically tried to create a colloidal and water soluble hydroxyapatite (nHA) nanocomposite using biologically active casein polymers as a matrix. [2-4]. Caseins are amphiphilic self-assembled proteins stable in aqueous solutions known as casein micelle. Their main biological function is the transport and delivery of proteins in the body. Noting that synthesis of nHA nanoparticles in casein substrate will be associated with certain technical difficulties because of its high tendency to aggregate. For reducing the size of nanoparticles ultrasonic treatment of the synthesis batch or addition a modifier agent have been applied. [5-7] Different methods which have been reported for preparation of the synthetic nHA were micro emulsion technique [8], wet chemical precipitation method [9], biomimetic preparation [10], sol–gel method [11], etc. Among these method, the

* Corresponding Author Email: *m.s.sadjad@gmail.com*

most widely used technique for synthesis of HA nanoparticle was chemical inverse micro emulsion method [12] which we have used it to prepare nHA colloidal system using different concentration of the main milk protein, casein.

EXPERIMENTAL

Material

All the starting chemical materials used in this work, $Ca(NO3)_2.4H_2O$, $(NH_4)_2HPO_4$, NaOH and cyclohexane were supplied from Merckcompany and used without any further purification. Casein proteinswere prepared in our Laboratory using commercial skimmed milk.

Isolation of Casein from Milk

50 ml skimmed milk was poured into a flask placed in a water bath heated to reach a critical temperature (40 °C). By addition 20 drops of acetic acid to the prepared sample and stirring with a glass rod, a clot of casein was obtained in the flask. The clots was separated from the mixture by vacuum filtration and added 25 ml of ethanol and stirred slowly to obtain dispersed casein in ethanol. To remove any remained impurities in the sample, the slurry was washed by 50 ml of a mixture of 1 : 1 ethanol / diethyl ether and dried at room temperature.

Synthesis of Hydroxyapatite nanocomposite

10 mL of aqueous solution of $(NH_4)_2HPO_4$ (0.6 M) was directly added to a reverse micro emulsion system prepared by dispersion of 0.1, 0.2 and 0.3g of our prepared casein powder in 30 ml cyclohexane under vigorous stirring batch. By injecting slowly 10 mL of appropriate aqueous solution of $Ca(NO_3)_2.4H_2O$ in the above prepared mixture and stirring again for about 15 minutes, a transparent solution was obtained. To adjust the pH in the range of 9-10, a small amount of NaOH solution (1M) was added to the system and vigorously stirred at room temperature for one day. The colloidal solutions (with and without biopolymer) were centrifuged and dried at 80 °C for 48 hrs.

Physical Characterization

Characterization of as prepared products was performed using XRD patterns using Philips expert pro. Diffractometer equipped with Cu_{Ka} radiation (λ=0.154 nm). The typical groups of the synthesized powders was analyzed by Fourier transform infrared spectroscopy (FT-IR, Model Thermo Nicolet's Nexus 870), in the wave number range of 400-4000 cm^{-1}, with a resolution of 4 cm^{-1}. Field Emission Scanning Electron Microscopy (FESEM) technique (MIRA3TESCAN-XMU) and Transmission Electron Microscopy (TEM) were used to examine and estimate the size, distribution and morphology of the samples (Zeiss-EM10C-100 KV). Particle size of HA/casein nanoparticles was measured using Dynamic Light Scattering (DLS) technique (ZS/ ZEN3600 Zeta sizer; Malvern, Instruments Ltd, Malvern, UK). This system was equipped with a 4 mV helium/neon laser at 633 nm wavelength and measures the particle size with the noninvasive back scattering technology at a detection angle of 173° after an at least 100-fold dilution with purified water. All of the DLS measurements were performed at 25.0 °C ± 0.1 °C at 20-second intervals for three repeat measurements. For zeta potential measurement, each diluted nanoparticle suspension was put in a universal folded capillary cell equipped with platinum electrodes. The electrophoresis mobility was measured and the zeta potential (ζ) was calculated by the Dispersion Technology Software provided by Malvern.

RESULTS AND DISCUSSION

X-Ray Diffraction (XRD) study

Fig. 1 shows XRD diffraction patterns of as prepared sample, at the presence of: a) 0.1g, b) 0.2g and c) 0.3 g Casein. All the main diffraction peaks recorded at (002), (211), (310), (222), (213) and (304) plane, were characteristic of the monophasic low crystalline HA with ICDD PDF No: 00—001-1008, matching well with the hexagonal system (P63/m). Very interesting point in this figure was appearance of the broad peaks width for the samples with different concentration of casein and a sample's broadening peak's width is in general a good evidence for explaining formation of nanostructured materials at the presence of a substrate. Average HA crystalline size was calculated using Scherrer`s [13] equation as follows:

$$D = K\lambda/\beta_{1/2}\cos\theta$$

Where, D is the average crystal size, K is a constant (here chosen as 1); λ is the wavelength of X-ray radiation (1.54056 A), $\beta_{1/2}$ is the half width of the diffraction peak and θ (°) is Bragg angle. The result of D values calculation for the samples prepared at the presence of 0.1, 0.2 and 0.3 g of casein were 13, 8 and 6 nm. This

crystalline size reduction can be explained by the effect of casein concentration on the crystalline size. Because, for an emulsion polymerization, higher amount of the surfactant can stabilizes smaller emulsion droplets because of their larger specific surface area.

FTIR Spectroscopy Study

Functional groups associated with hydroxyapatite were identified by FTIR spectroscopy. Recorded FTIR spectrum for the sample synthesized in the presence of 0.3 g casein is given in Fig. 2. In this figure, the presence of hydroxyl group in the apatite lattice is well confirmed by absorption broad bands at 3571 cm^{-1} and 629 cm^{-1}, attributed to the stretching and flexural modes of hydroxyl (OH^-) group. The IR characteristic peaks of phosphate groups appeared between 1090-1030 and 600-560 cm^{-1}originated from bending and stretching vibration mode of phosphate of HAp respectively [14-15]. The absorption bands at 1420 cm^{-1} and 875 cm^{-1} suggest the presence of CO_3^{-2} in hydroxyapatite structure [16]. Likewise, the other stretching vibrations for carbonyl and phosphate groups were also observed as reported. The peaks appearing at 2924 $cm^{-1,}$ 2854 cm^{-1} and 2956 cm^{-1} are assigned to the vibrating absorption of C-H asymmetric and symmetric stretching in CH_2 and C-H asymmetric stretching in CH3 respectively [17]. All peak's assignment were shown in Table 1.

The FE-Scanning electron microscopy

Fig. 3 shows FE-SEM micrograph for the sample prepared on 0.3 g casein in micro emulsion system. In this image, formation of homogeneous distribution of uniform spherical nanoparticles aligned in a rod like system can be distinguished.

The Transmission electron microscopy

Fig. 4 shows TEM image of the as prepared sample at the presence of 0.3 g casein. This image reveals formation of needle like morphology of HA nanoparticles with a mean crystalline size of approximately 10 nm in diameter and 60-70 nm in length. This value is much more different than of the crystallite size obtained via Scherrer's equation. This discrepancy between crystalline and grain size can be due to the effect of casein addition as scaffold in the batch preparation to provide the necessary condition for formation grain size nHA at room temperature. Interesting point in this image was arrangement of the needle like HA around spherical casein micelles (shown in circle at Fig. 4).

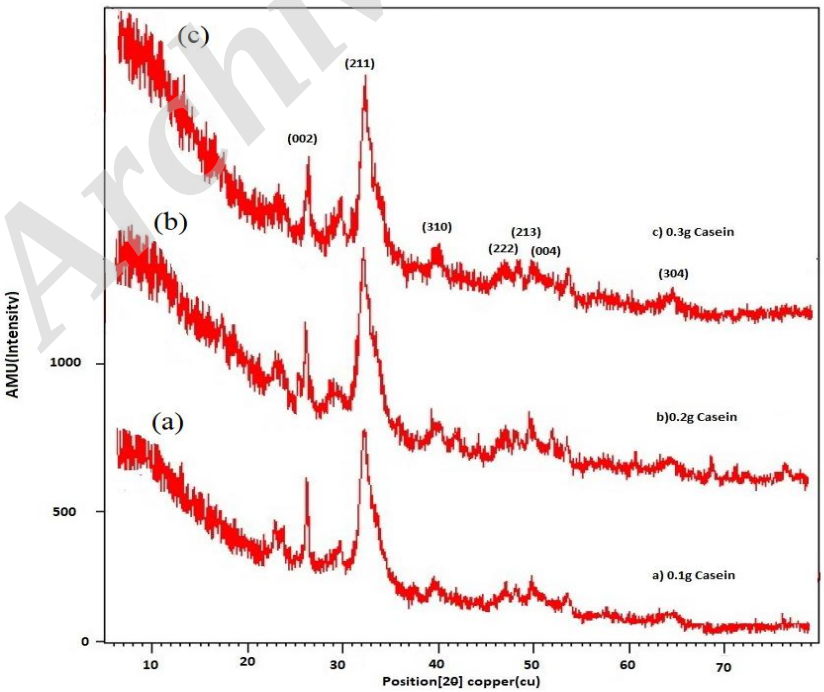

Fig. 1: XRD patterns of as-prepared nHA nanoparticles at the presence of: a) 0.1 g casein; B) 0.2 g casein; and C) 0.3 g Casein.

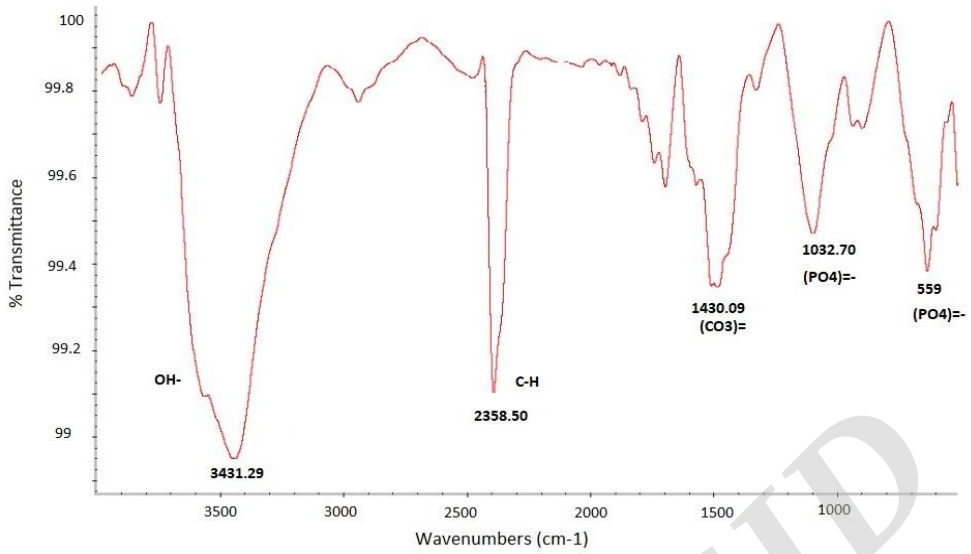

Fig. 2: FTIR spectra of nHA prepared in the presence of 0.3g casein.

Table 1: The peaks assignment for FTIR spectrum of nHA, nHA/Casein.

	nHAp(cm^{-1})	Mode	nHAp+0.1g Casein (cm^{-1})	nHAp+0.2g Casein (cm^{-1})	nHAp+0.3g Casein (cm^{-1})
PO_4^{3-}	570.89	υ_4 bending	562	556	559
	601.74		611	668	670
	1049.2	υ_3 vibrational	1041	1043	1032
OH^-	3571.92	bending vibration H_2O	3426	3423	3431
	1630		1641	1642	1646
	1458.08		1448	1450	1430
	876		874	873	829
C-H	3000-2800	casein	2918	2921	2920
N-H	3600-3400	casein	3868, 3743	3856, 3742	3860, 3742

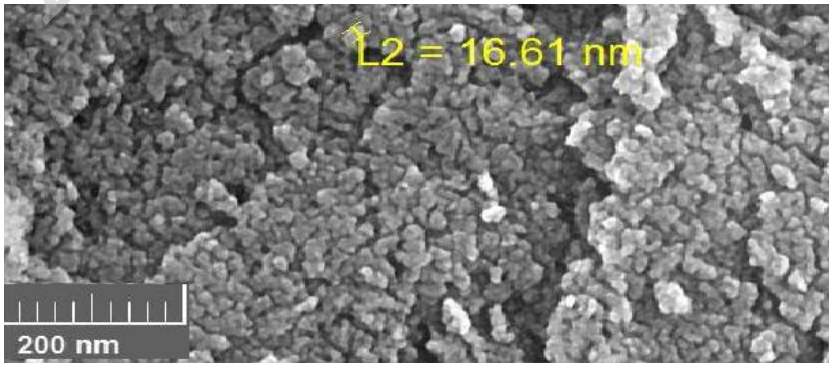

Fig. 3: FE-SEM images of nHA prepared in the presence of 0.3 g casein.

Particle size and zeta potential distributions

Dynamic light scattering (DLS) is a valuable tool for studying size and degree of agglomeration of the nanoparticles as a function of time in the suspension solution. In this technique, one can determine hydrodynamic size of the nanoparticles by measuring intensity of laser scattered light that passes through a colloidal solution. Larger particles will diffuse slower than smaller particles. So, particle size can be mathematically provided by measuring time dependence of the scattered light. The DLS experimental data obtained in this work which is given in Fig. 5 shows a zeta particle size distribution of 265.6 nm. In fact, this is the average particle size of the hydrodynamic colloidal nanoparticle in HA/casein suspension. Simulated image of this particle size distribution (6a) which is supported by TEM image of nHA prepared at the presence of 0.3 g casein is presented in Fig. 6b.

The zeta-potential of the particles which is a basic parameter in controlling stability of colloidal suspensions is obtained by measuring particles mobility under an applied electric field which is applied and can be calculated using Smoluchowski equation [18]:

$$Z = \frac{\eta}{\varepsilon_0 \varepsilon_r} U$$

Where, and are dielectric constants of vacuum and solvent respectively, η is viscosity and U is the mobility of the particles in suspended solution. In general, when an electric field is applied to the charged particles in a colloidal sample, particles move toward an electrode opposite to its surface charge. Because the velocity is proportional to the amount of charge of the particles, zeta potential can be therefore estimated by measuring the mobility of these particles. To determine the speed of the particles movement, the particles was normally irradiated with a laser light, and the light emitted from the particles was detected from the shifted scattered frequency. Since, shifted scattered light from incident light is proportional to the speed of the particles movement, and the electrophoretic mobility of the particles can be thereby measured [19-21]. The most widely used theory for calculating zeta potential from experimental data was developed by Marian Smoluchowski in 1903 [22]. Experimental zeta potential value obtained in this work for ionically cross linked HA/casein suspension is given in Fig. 7 This result reveals a bimodal zeta potential distribution may be due to the two different populations of particles within the prepared suspension sample. About 42% of the particles have a zeta potential of +23 mV, and 58% of the particles have a lower value of +2.94 mV. Considering that and a dividing line between stable and unstable aqueous dispersions reported at either +30 or -30mV, particles with zeta potentials more positive than +30mV have been considered stable and particles with low absolute values of the zeta potential will agglomerate and the dispersion becomes unstable [23-31], we can conclude that colloidal samples prepared in this work at the our experimental condition even after 4 hours ultrasonic treatment, were unstable because of casein- calcium high tendency to aggregate. To assure stabilized colloidal suspensions, addition of some anticoagulant agent to regulate stability of the colloidal suspensions seems to be indispensable.

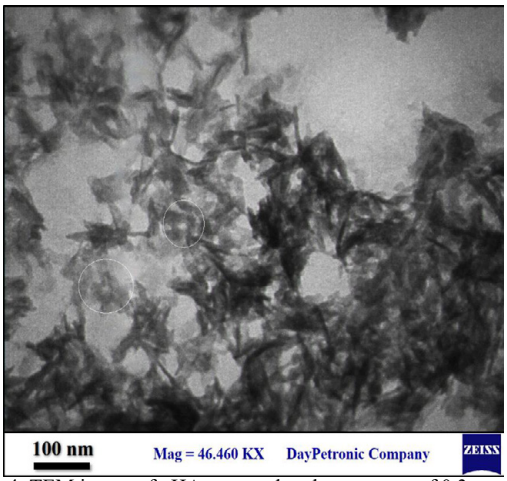

Fig. 4: TEM image of nHA prepared at the presence of 0.3g casein.

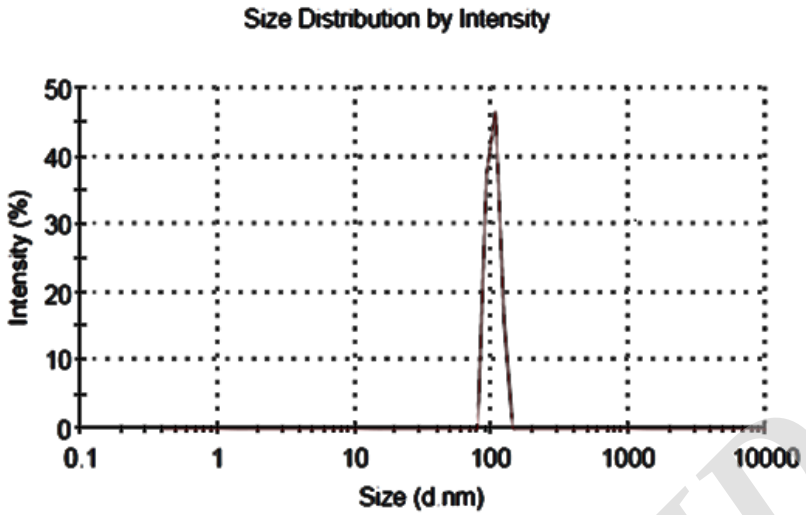

Fig. 5: DLS measured results for colloidal HA as prepared on 0.3g casein.

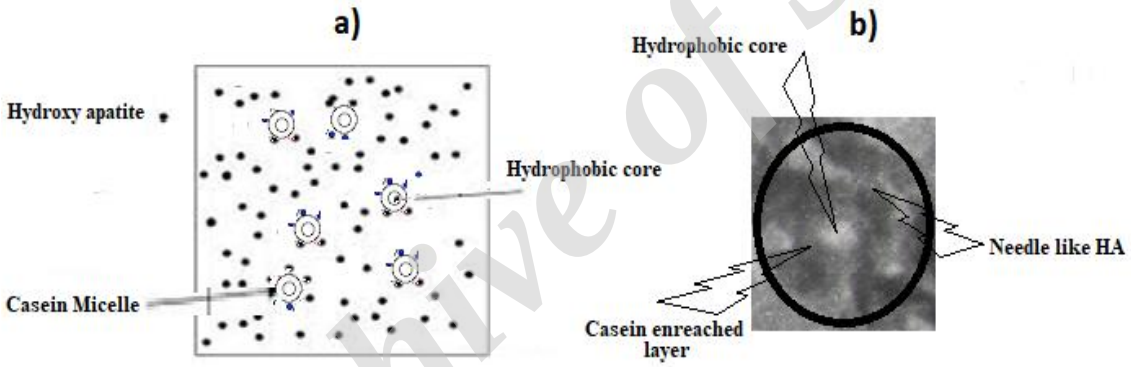

Fig. 6: Simulated representation of hydrodynamic colloidal particle size distribution of HA/casein (a) TEM image of nHA prepared at the presence of 0.3g casein (b).

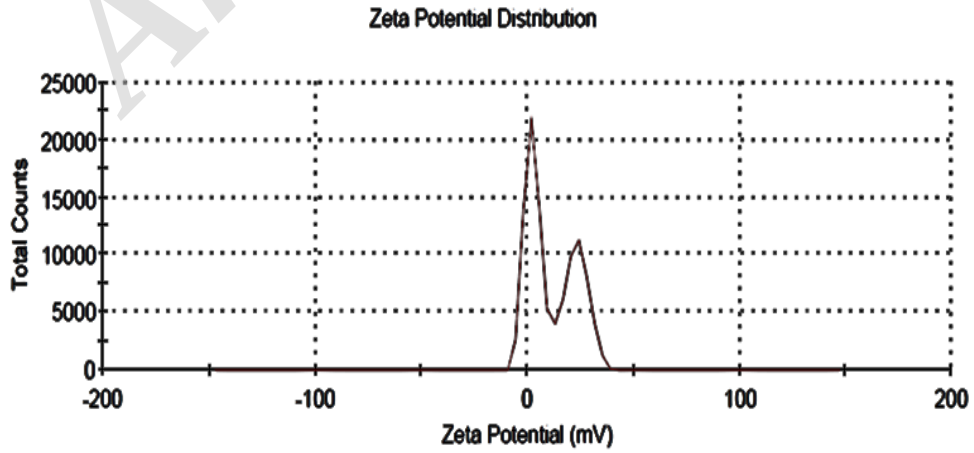

Fig. 7: Zeta potential distributions forcolloidal HA nanoparticlesas prepared in the presence of 0.3 g casein.

CONCLUSION

HA nanoparticles were successfully prepared in an inverse micro emulsion template phase consisting of cyclohexane, water, anionic surfactant and co-surfactant. The X-ray diffraction patterns confirmed formation of hexagonal nHA crystalline at the presence of casein micelles. Arrangement of needle like HA crystallite at around casein micelles in its colloidal solution, was clearly evidenced by TEM image. Dynamic light scattering (DLS) techniques used to measure particle size and zeta potential distribution revealed successful preparation of a colloidal HA/casein suspension with a hydrodynamic size distribution of 256.6 nm. Bimodal zeta potential distribution in divergence with the DLS average zeta size data reveals unstability of the colloidal HA/casein suspension because of casein- calcium nanocomposite's high tendency to aggregation.

ACKNOWLEDGMENTS

We would like to thank research vice presidency of Science and Research Branch of Islamic Azad University for providing financial support.

CONFLICT OF INTEREST

All authors declare no conflicts of interest in this paper.

REFERENCE

[1] Eriksson M., Liu Y., Hu J., Gao L., Nygren M., Shen Z., (2011), Transparent hydroxyapatite ceramics with nanograin structure prepared by high pressure spark plasma sintering at the minimized sintering temperature. *J. Eur. Ceram. Soc.* 31: 1533-1538.

[2] GrossinD., Rollin-Martinet S., Estournès C., Rossignol F., Champion E., Combes C., Rey C., Geoffroy C., Drouet C., (2010), Biomimetic apatite sintered at very low temperature by spark plasma sintering: Physico-chemistry and microstructure aspects. *Acta Biomater.* 6: 292-299.

[3] Severin A. V., Bozhevolnov V. E., Smykov I. T., (2014), The means of hydroxyapatite nanoparticles (n-HAP) preparation in biopolymer modifiers solutions under ultrasonic activation have been investigated. *Allerton Press Inc.* 69: 45- 48.

[4] Li S., Izui H., Okano M., Zhang W., Watanabe T., (2008), Processing and properties of advanced ceramics and composites. *Mater. Sci. Technol. Conf. Pennsylvania,* 93.

[5] Paz A., Guadarrama D., López M., González J. E., Nayrim Brizuela N., Aragón J., (2012), A Comparative study of hydroxyapatite nanoparticles synthesized by different routes. *J. Quim. Nova*. 23: 1724-1727.

[6] Rodríguez-Lugo V. Salinas-Rodríguez E. Vázquez R. A., Alemán K., Rivera A. L., (2017), Hydroxyapatite synthesis from a starfish and β-tricalcium phosphate using a hydrothermal method. *RSC Adv.* 7: 7631-7639

[7] Ferraz M. P., Monteiro F. J., Manel C. M., (2004), Hydroxyapatite nanoparticles: A review of preparation methodologies. *J. Appl. Biomater. Biomech.* 2: 74-80.

[8] Severin A. V., Badun G. A., Chernysheva M. G., (2011), Studying the nature of interaction between nanohydroxyapatite and albumins by radionuclide-microscopy diagnostics. *Moscow Univ. Chem. Bull.* 66: 371-376.

[9] Seyed Sadjadi M. A., Akhavan K., Zare K., (2011), Preparation of hydroxyapatite nanoparticles by reverse microemulsions and polyelectrolyte-modified, Microemulsions. *Res. J. Chem. Environ.* 15: 959-962.

[10] Eslami H., Solati-Hashjin M., Tahriri M., (2008), Synthesis and characterization of hydroxyapatite nanocrystals via chemical precipitation technique. *Iranian J. Pharmaceut. Sci. Spring.* 4: 127-134.

[11] Zhao F., Yina Y., Lu W. W., Leong J. C., Zhang W., Zhang J., Zhang M., Yao K., (2002), Preparation and histological evaluation of biomimetic three-dimensional hydroxyapatite/chitosan-gelatin network composite scaffolds. *J. Biomater. Sci.* 23: 3227-3234.

[12] Bilton M., Brown A. P., Milne S. J., (2010), Sol-gel synthesis and characterisation of nano-scale hydroxyapatite. *J. Phys. Conf. Ser.* 241: 012042.

[13] Mobasherpour I., Heshajin M. S., Kazemzadeh A., Zakeri M., (2007), Studies on processing and characterization of hydroxyapatite biomaterials from different bio wastes. *J. Alloys Comp.* 430: 330-333.

[14] Najafizadeh F., SeyedSadjadi M. A., Fateami S. J., Mobarakeh M. K., Afshar R. M., (2016), The effects of silica and a nature polymer on the size and properties of nanohydroxyapatite. *Hacettepe J. Biol. Chem.* 44: 317-325.

[15] Cullity B. D., (1978), Elements of X-ray diffraction. Reading, MA: Addison-Wesley.

[16] Gergely G., Wéber F., LukácsI., Illés A. L., Tóth Z. Horváth E., Mihály J., Balázsi C., (2010), Nanohydroxyapatite preparation from biogenic raw materials. *Central Europ. J. Chem.* 8: 375-381.

[17] Ghosh S. K., Prakash A., Datta S., Roy S. K., Basu D., (2010), Effect of fuel characteristics on synthesis of calcium hydroxyapatite by solution combustion route. *Bulletin of Mater. Sci.* 33: 7-16.

[18] Rodríguez-Lugo V., Salinas-Rodríguez E., Vázquez R. A., Alemán K., Rivera A. L., (2017), Hydroxyapatite synthesis from a starfish and β-tricalcium phosphate using a hydrothermal method. *RSC Adv*. 7: 7631-7639.

[19] Shahmohammadi M., Jahandideh R., Behnamghader A., Rangie M., (2010), Sol-gel synthesis of FHA/CDHA nanoparticles with a nonstochiometric ratio. *Int. J. Nano Dimens.* 1: 41-45.

[20] Wang J. P., Chen Y. Z., Yuan S. J., Sheng G. P., Yu H. Q., (2009), Synthesis and characterization of a novel cationic chitosan-based flocculant with a high water-solubility for pulp mill wastewater treatment. 43: 5267-5275.

[21] De Bruyn J. R., Goiko M., Mozaffari M., Bator D., Dauphinee R. L., (2013), Dynamic light scattering study of inhibition of nucleation and growth of hydroxyapitate crystals by osteopontin. *Plus One.* 8: 56764-56768.

[22] Lyklema J., (1995), Fundamentals of interface and colloid science. 2: 3-208. ISBN 0-12-460529-X.

[23] Russel W. B., Saville D. A., Schowalter W. R., (1992), Colloidal dispersions, cambridge university press. ISBN 0-521-42600-6.

[24] Dukhin A. S., Goetz P. J., (2002), Ultrasound for characterizing colloids. Elsevier. ISBN 0-444-51164-4.

[25] Hunter R. J., (1989), Foundations of colloid science, Oxford University Press. ISBN 0-19-855189-4.

[26] Smoluchowski M., (1903), Contribution to the theory of electro-osmosis and related phenomena. *Bull. Int. Acad. Sci. Cracovie.* 3: 184-199.
[27] Morrison I. D., Ross S., (2002), Colloidal dispersions: Suspensions, emulsions, and Foams. ISBN 978-0-471-82848-8.
[28] Wang L., Li S., (2012), Phosphorylated osteopontin peptides inhibit crystallization by resisting the aggregation of calcium phosphate nanoparticles. *Cryst. Eng. Comm.* 14: 8037-8043.
[29] Sadjadi M. S., Meskinfam, M., Sadeghi B., Jazdarreh H., Zare K., (2010), In situ biomimetic synthesis, characterization and in vitro investigation of bone-like nanohydroxyapatite in starch matrix. *Mat. Chem. Phys.* 124: 217-222.
[30] Sadjadi M. S., Meskinfam, M., Sadeghi B., Jazdarreh H., Zare K., (2011), In situ biomimetic synthesis and characterization of nano hydroxyapatite in gelatin matrix. *J. Biomedical Nanotech.* 7: 450-454.
[31] Sadeghi B., Ghammamy Sh., Gholipour Z., AminiNia A., (2011), Gold/hydroxypropyl cellulose hybrid nanocomposite constructed with more complete coverage of gold nano-shell. *Mic. & Nano Lett. IET.* 6: 209-213.